

# SIMPLIFIED EXPRESSIONS FOR MODELLING RIGID ROCKING STRUCTURES ON TWO-SPRING FOUNDATIONS

Quincy T. Ma<sup>1</sup> and John W. Butterworth<sup>2</sup>

*This paper was presented at the 2010 NZSEE Annual Conference in Wellington.*

## SUMMARY

This paper presents a new technique for modelling the dynamic response of uplifting rigid structures subjected to base excitation. The proposed technique exploits the use of a two-spring foundation, and subsequently an equivalent single-degree-of-freedom procedure is established to model the dynamics of the system. A set of simplified closed-form expressions have been developed to estimate the system's restoring force-displacement characteristics. The simplified expressions only require details of the system geometry and are shown to predict the nonlinear force-displacement characteristics of a rocking structure as closely as those determined from a complicated pushover analysis.

This paper presents two additional numerical examples to demonstrate the use of the proposed technique to simulate the displacement time-histories of a prototype structure under free-vibration-decay or when subjected to earthquake excitations.

## INTRODUCTION

Rocking motion is a commonly observed phenomenon with complex and nonlinear behaviour. It can be shown that by allowing rocking motion to take place in structures, the resulting accelerations and hence forces can be significantly reduced. This approach when applied correctly acts as an effective isolation mechanism for structures against severe ground motion. A rocking solution yields little increase, and often a decrease in construction cost, while substantially enhancing the seismic resistance of structures and their post-earthquake serviceability.

Modern researchers have suggested that the ancient Greeks may have deliberately designed their columns to rock in strong ground motions contributing to the survival of many ancient structures (Pampanin 2006; Psycharis *et al.* 2000). More recent examples of modern major structures utilising rocking for seismic isolation include the South Rangitikei Viaduct in New Zealand, the Northern approach of the Lions Gate Bridge in Vancouver, Canada and the Rio Vista Bridge in Sacramento, California (Beck and Skinner 1974; Palmeri and Makris 2008; Tse *et al.* 2002).

A prevalent sentiment amongst practitioners is that although the philosophy behind rocking as a seismic isolation solution is logical, it is prudent not to implement it for high seismic areas until the system performance has been tested by an actual major earthquake (Arze 1993).

Another impediment to the adoption of rocking as an isolation technique is the lack of available guidelines for engineers. This has been partly addressed recently in a paper by Kelly (2009) as part of a recent EQC funded research project.

## IMPORTANCE OF AN IMPACT MODEL AND ROCKING INTERFACE ASSUMPTION

A key challenge in the modelling of rocking motion is arguably the unification of two phenomena which occur at very different time scales. These two dissimilar phenomena are 1) the relatively long-duration smooth rocking motion, and 2) the infinitesimal-duration impact events which occur whenever a rocking object returns to or passes through the upright position.

The transition between the two phenomena is usually facilitated by an impact model. An impact model predicts the initial conditions of the post-impact motion given the conditions of system immediately prior to the impact. In the simplest sense, the post-impact motion is fully specified by two variables, 1) the centre of rotation location, and 2) the angular speed of the system.

For example, consider a rigid block under general rocking motion at the instant it impacts the ground as in Figure 1. The block has an instantaneous angular speed  $\dot{\theta}^+$  and a tangential velocity of  $\tilde{v}_G^+$  at the centre of gravity about some arbitrary centre of rotation  $C^+$ . The role of the impact model is then to provide an estimation of the new instantaneous angular speed  $\dot{\theta}^-$ , tangential velocity  $\tilde{v}_G^-$  and the location of the new centre of rotation  $C^-$  after the impact.

---

<sup>1</sup>Lecturer, Department of Civil and Environmental Engineering, The University of Auckland, Auckland (Member)

<sup>2</sup>Associate Professor, Department of Civil and Environmental Engineering, The University of Auckland, Auckland (Member)

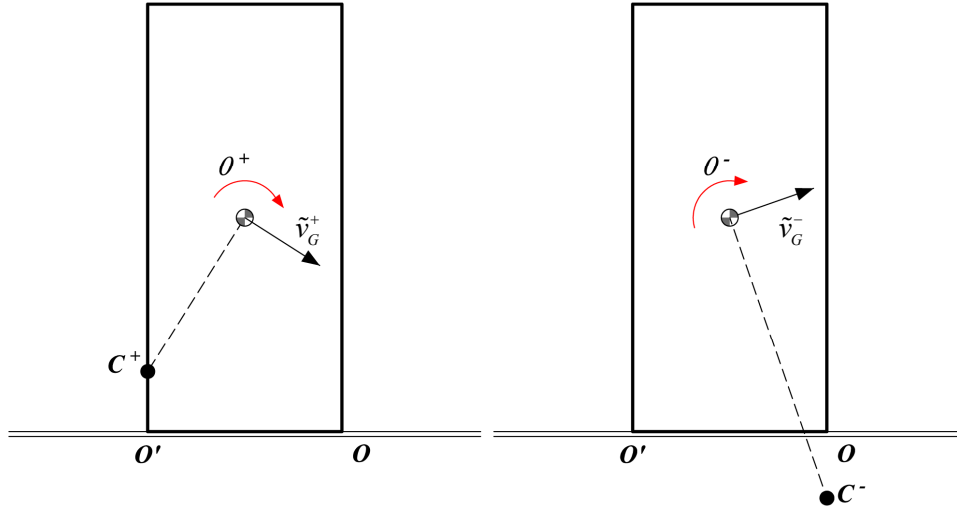


Figure 1: Key parameters for an impacting rocking object.

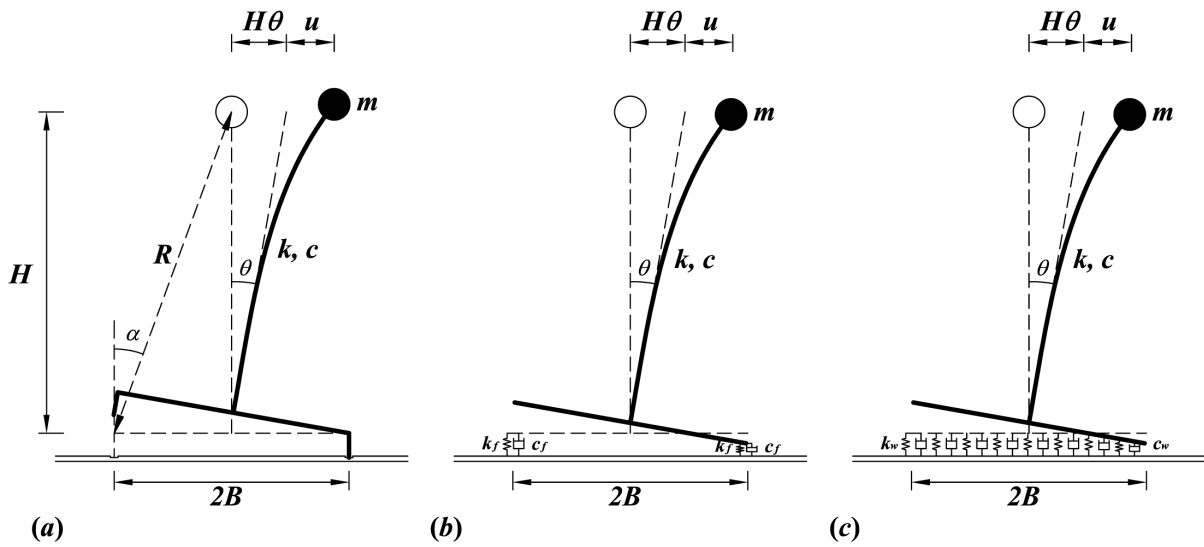


Figure 2: Three categories of rocking interface assumption.

In practice, it is very difficult to predict exactly the location of the centre of rotation and the exiting angular speed after a rocking impact. This is due to a large number of uncertainties involved in the impact problem. These include the exact contact area, the duration of the impact and the energy lost due to the impact. As a result, researchers have typically made assumptions on one or both of the governing variables of the post rocking-impact motion. For instance, the plastic impact assumption in Housner's simple rocking model (SRM) restricts the post-impact motion to be purely rotational about the point of application of the impulsive force (Housner 1963). This point of application is assumed to have an infinitesimal area, and consequently, assuming no bouncing will occur, the exiting angular speed can be derived through the conservation of angular momentum about the impact point.

Thus, the plastic impact assumption completely prescribes the post-impact motion by imposing both the centre of rotation location and the exiting angular speed. The plastic impact model in Housner's SRM also implicitly prescribes the energy dissipation from a rocking impact.

Researchers have also circumvented the impact problem altogether by enforcing continuity throughout the transitions between smooth rocking and the impact event. This is generally done by the insertion of a compression-only visco-elastic layer between the rocking system and the ground. Researchers rationalised this form of solution on the basis that real rocking structures rest on soils and foundations which have a finite stiffness.

The treatment of rocking impacts and assumptions of the rocking interface properties neatly divide the existing studies on the behaviour of flexible structural systems with foundation uplift into three categories:

- A. Studies that assume the rocking interface is rigid, resulting in Housner's plastic impacts and fixed rocking pivots assumptions (Ichinose 1986; Meek 1975; Psycharis 1991).
- B. Studies that assume the rocking interface is flexible but the locations of rocking pivots are fixed (Huckelbridge and Clough 1978; McManus 1980; Psycharis 1991; Sharpe and Skinner 1983; Xu and Spyarakos 1996; Yim and Chopra 1984b; Yim and Chopra 1985).
- C. Studies that assume the rocking interface is flexible and can be represented by a bed of independent compression-only springs, or otherwise known as a Winkler foundation. This implicitly allows for spatially varying rocking pivots, a continuous support force and the possibility of planar impacts (Anderson 2003; Yim and Chopra 1984a).

These three approaches are illustrated diagrammatically in Figure 2.

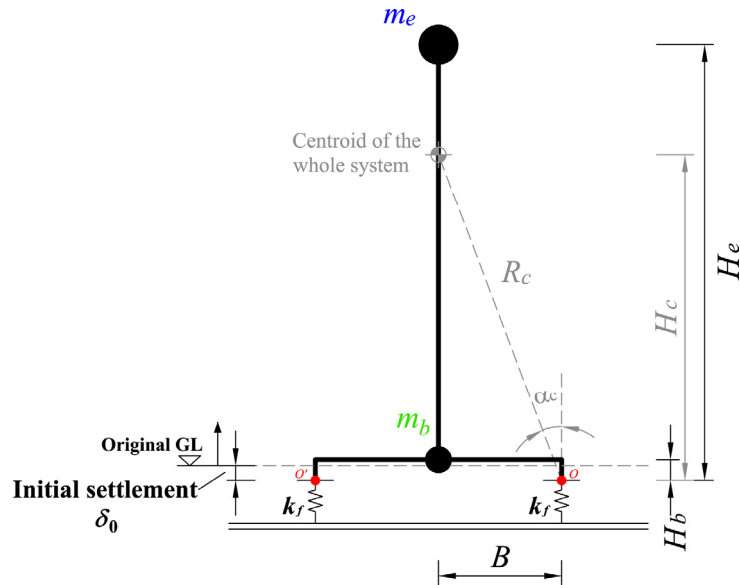


Figure 3: Rigid lumped-mass rocking structure on two-spring foundation.

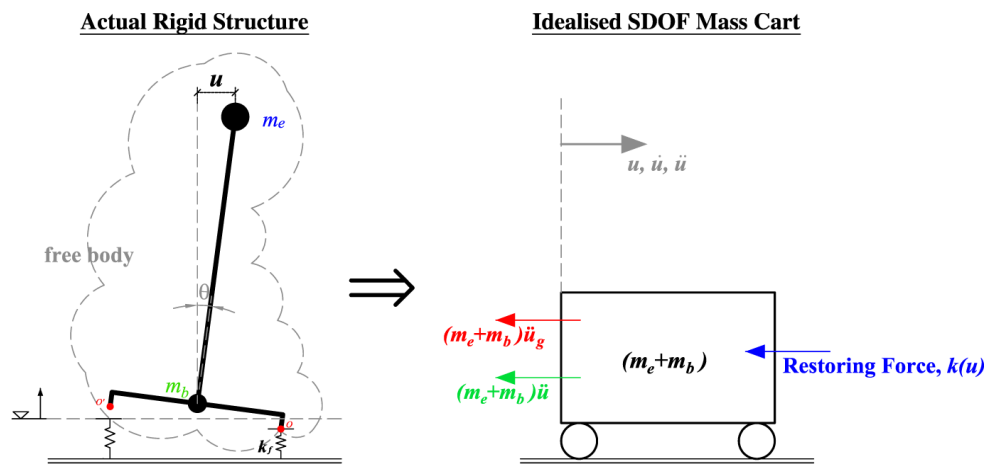


Figure 4: The idealised SDOF mass cart.

## A RIGID LUMPED-MASS ROCKING STRUCTURE ON A TWO-SPRING FOUNDATION

### Model definitions

The current study aims to simplify aspects of the two-spring foundation approach for analysing uplifting structures. The study places an emphasis on the lateral load resisting capacity arising from a rocking mode only. Consequently, the structure is modelled as a single effective lumped-mass ( $m_e$ ) located at the mass centroid of the structure. This effective lumped-mass is in turn connected to another lumped-mass ( $m_b$ ), representing a rigid footing, by a rigid link. The latter lumped-mass represents the mass of the footing and is located at the assumed mass centroid.

The idealised rigid structure rests on two compression-only springs that are located at the edge of the rigid footing. This arrangement is herein referred to as the two-spring foundation, and an illustration of the setup is presented in Figure 3

The two-spring foundation simulates the compliance of the supporting ground through an empirically selected spring stiffness value ( $k_f$ ). This spring arrangement facilitates a gradual transfer of support forces from one support to the other prior to the initiation of uplift. This in effect assumes the rigid structure rotates about its centreline until liftoff occurs in one of the compression-only springs. After liftoff occurs, the structure rotates about the spring which is still in contact.

It is noteworthy that the two-spring foundation in this model lacks a viscous damper like that in the conventional studies. This is because energy dissipation from impacts will be implemented by modifying the post-impact conditions directly, instead of the conventional emulation through viscous damping. This approach specifies the amount of energy dissipation more precisely and the energy dissipation occurs instantly, which is arguably more compatible with the actual event.

This model shares three key assumptions with Housner's SRM, which are 1) sliding is prohibited, 2) the sole source of energy dissipation is through impacts, and 3) impacts are plastic and hence no bouncing is permitted.

### A simplified nonlinear single-degree-of-freedom dynamic model

While it is relatively simple to analyse a specific problem adopting the two-spring foundation using finite element techniques, such endeavours only provide solutions on a case-by-case basis and little insight into the behaviour of the systems in general. Accordingly, this study establishes a simplified model to enable the study of rocking systems more generally.

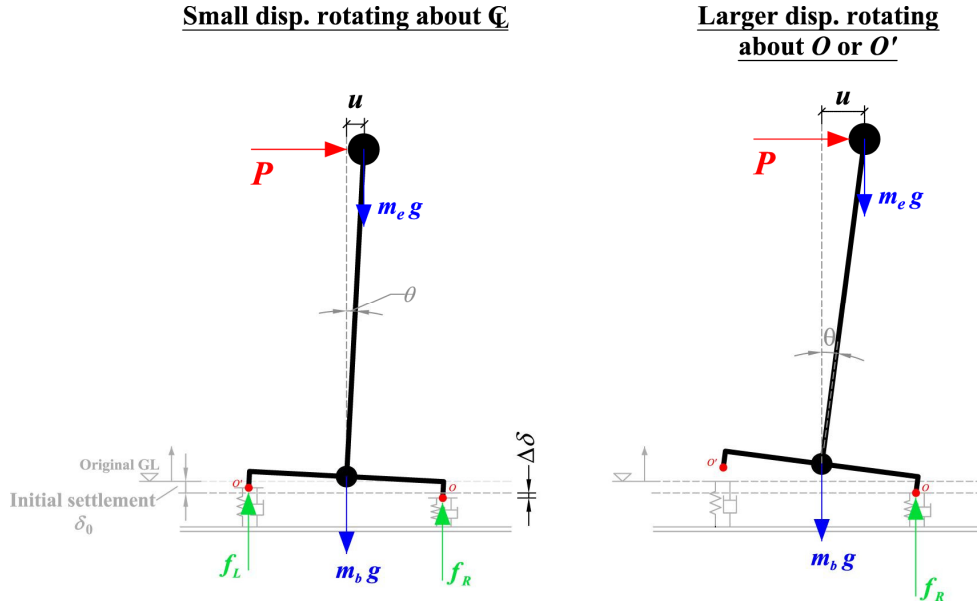


Figure 5: Force diagrams of the rocking structure subjected to increasing displacements.

Taking advantage of the rigid body assumption, the system is simplified as a nonlinear single-degree-of-freedom (SDOF) system with the displacement of the top mass ( $u$ ) as the only active degree-of-freedom. An analogy is considering the rocking system as a SDOF mass cart is as shown in Figure 4.

Applying D'Alembert's principle, the equivalent system is in a static equilibrium. A summation of forces in the direction of  $u$  gives rise to the governing differential equation (GDE) of motion in Equation 1. This is subsequently integrated numerically to predict the displacement time-history of a rocking system.

$$(m_e + m_b)\ddot{u} + k(u) = P(t) \quad (1)$$

where  $k(u)$  = Nonlinearly elastic restoring force-displacement characteristics of the rocking system;  
 $P(t)$  = Driving force of the system, equals  $-(m_e + m_b)\ddot{u}_g$  when the forcing is a result of ground acceleration  $\ddot{u}_g$ .

It is noteworthy that the inertial term of the system is taken as  $(m_e + m_b)\ddot{u}_g$  even when the two lumped-masses appear to experience different accelerations. This is justified as the system is simplified as an effective free body, and the rigid body geometric nonlinearity is represented in the nonlinear restoring force-displacement relationship. The role of the inertial term is to ensure it gives rise to a correct base shear under unit acceleration.

Radiation damping from rocking impacts is assumed to be the sole source of energy dissipation in the SDOF dynamic model. The numerical integration is stopped whenever an impact is detected, then restarted with the velocity of the system reduced according an apparent coefficient of restitution ( $r$ ) as in Equation 2. In this study, impacts are deemed to take place when  $u = 0$  for convenience. A theoretical expression for  $r$  can be developed assuming the conservation of angular momentum about the point of impending contact immediately before and after an impact. The expression for the two-mass model is presented as Equation 3.

$$r = \frac{\left(\frac{\dot{\theta}_2}{\dot{\theta}_1}\right)^2}{\left(\frac{\dot{u}_2}{\dot{u}_1}\right)^2} \quad (2)$$

$$r = \frac{\left[ \frac{m_e(H_e^2 - B^2) + I_{e,g}}{m_e(H_e^2 + B^2) + I_{e,g}} + \frac{m_b(H_b^2 - B^2) + I_{b,g}}{m_b(H_b^2 + B^2) + I_{b,g}} \right]^2}{\left[ \frac{m_e(H_e^2 - B^2) + I_{e,g}}{m_e(H_e^2 + B^2) + I_{e,g}} + \frac{m_b(H_b^2 - B^2) + I_{b,g}}{m_b(H_b^2 + B^2) + I_{b,g}} \right]^2} \quad (3)$$

where  $\dot{\theta}_1, \dot{\theta}_2$  = Angular speed of the system before and after an impact respectively; and

$\dot{u}_1, \dot{u}_2$  = Horizontal speed of the system before and after an impact respectively.

$m_e, m_b$  = Mass of the effective lumped-mass representing the structural system and the base structure respectively;

$I_{b,g}, I_{e,g}$  = Moment of inertia of the footing and the structural system about their respective mass centroids respectively; and  $B, H_b, H_e$  are as defined in Figure 3.

### Nonlinear static force-displacement relationship

A key component required for predicting the displacement time-history is establishing the equivalent restoring force-displacement relationship of the rocking system,  $k(u)$  in Equation 1. The role of  $k(u)$  is to reproduce the overall restoring force of the equivalent SDOF system, arising from the geometrically nonlinear path of the system's weight force as the system rocks. The result is a nonlinear function in terms of the lateral displacement only.

One possible way to obtain  $k(u)$  is by conducting a displacement-controlled pushover analysis of the actual system. This involves applying a varying pseudo-static lateral force at the top lumped-mass of the rigid structure, with the force applied slowly enough such that no dynamic effects are generated. Considering this process analytically, the inertial term in Equation 1 is deactivated and the restoring force  $k(u)$  is the pseudo-static lateral force required to satisfy equilibrium. Typically, the pseudo-static lateral force would be increasing, however it may also decrease so long as  $u$  is increased smoothly.

A set of simplified closed-form equations can be derived to describe  $k(u)$ . This is achieved by conducting an analytical pushover analysis for the general case. The derivation is as follows.

Consider the rigid rocking system at rest prior to the application of a lateral load ( $P$ ). The initial settlement of the rocking system ( $\delta_0$ ) on the two-springs can be evaluated by Equations 4 and 5.

$$\delta_0 = \frac{W}{2k_f} \quad (4)$$

$$W = (m_e + m_b)g \quad (5)$$

where  $g = \text{gravitational acceleration} = 9.81 \text{ ms}^{-2}$ .

Now consider applying a small lateral load to the right, such that the rigid structure rotates by an angle  $\theta$  and both ground springs remain in contact. The rigid structure rotates about its centreline and the support force is transferred from one spring to the other as illustrated in the force diagram in Figure 5a. During this time, the horizontal displacement is related to the rotation by Equation 6, and the change in spring length is approximated by Equation 7.

$$u = H_e \sin(\theta) \quad (6)$$

$$\Delta\delta \approx B \times \theta \quad (7)$$

Accordingly, the spring forces at the two supports in this scenario can be evaluated using Equations 8 and 9.

$$f_L = \frac{W}{2} - k_f B \theta \quad (8)$$

$$f_R = \frac{W}{2} + k_f B \theta \quad (9)$$

The transfer of support force continues as the lateral load ( $P$ ) is increased. This continues until the support force on the left spring reaches zero, when liftoff occurs. The rotation at which liftoff occurs, herein known as the critical rotation  $\theta_{crit}$ , can be estimated by substituting  $f_L$  equal to zero in Equation 8. This leads to expressions for estimating  $\theta_{crit}$  and the corresponding horizontal displacement ( $u_{crit}$ ) presented as Equations 10 and 11.

$$\theta_{crit} = \frac{W}{2k_f B} \quad (10)$$

$$u_{crit} = \frac{WH_e}{2k_f B} \quad (11)$$

Continuing to consider the scenario when both springs are still in contact with the structure, the applied force ( $P$ ) which causes a particular rotation ( $\theta$ ) can be estimated by considering moment equilibrium about the rotation centre, which is located at the intersection of the structure's centreline and the plane of the initial settlement. Assuming  $\theta$  is small, this leads to Equations 12 and 13.

$$P = \left[ \frac{2k_f B^2}{H_e} - g \left( m_e + m_b \frac{H_b}{H_e} \right) \right] \theta \quad (12)$$

$$P = \left[ \frac{2k_f B^2 - m_e g H_e - m_b g H_b}{H_e^2} \right] u \quad (13)$$

Equation 13 illustrates that the lateral restoring force increases linearly with increasing horizontal displacement when both springs are in contact. Furthermore, the lateral force causing liftoff can be estimated by substituting the expression for  $\theta_{crit}$ , Equation 10, into Equation 12. This is presented as Equation 14 below.

$$P_{crit} = \left[ \frac{WB}{H_e} - g \left( m_e + m_b \frac{H_b}{H_e} \right) \right] \frac{W}{2k_f B} \quad (14)$$

It can be shown that Equations 12 through 14 can be simplified by treating the two-mass system as a single lumped mass at the system centroid. This results in the following simplified formulae,

$$P = \left[ \frac{2k_f B^2 - WH_c}{H_e^2} \right] u \quad (15)$$

$$P_{crit} = \left[ \frac{2k_f B^2 - WH_c}{H_e^2} \right] u_{crit} \quad (16)$$

$$P_{crit} = \frac{W}{H_e} \left( B - \frac{WH_c}{2k_f B} \right) \quad (17)$$

$$\text{where } H_c = \frac{m_e H_e + m_b H_b}{m_e + m_b};$$

$$\alpha_c = \frac{B}{H_c}; \quad \text{and} \quad R_c = \sqrt{B^2 + H_c^2}.$$

Next, considering the case after liftoff has occurred, the rotation centre shifts to the compression spring that is in contact with the structure. From this point onwards, geometric nonlinearity becomes important and there is no further change in spring forces because of vertical equilibrium. This scenario is illustrated in Figure 5b.

Adopting the representation of the system with a single lumped-mass at the centroid, the restoring force of the rocking system can be evaluated by considering moment equilibrium about the rocking pivot. This leads to Equation 18 which prescribes the restoring force of the system as a function of the rotation.

$$P = W \frac{R_c \sin(\alpha_c - \theta)}{R_c \cos(\alpha_c - \theta)} \quad (18)$$

A closer examination of Equation 18 reveals the trigonometric term in the equation is effectively linear in  $\theta$  for a slender structure. This is convenient as there are two readily available fixed points on this curve which can be used to fit a linear approximation. The two points are i) the instant when uplift is initiated, and ii) the instant when the centroid of the system is directly above the pivot and the restoring force diminishes to zero.

Consider fixed point i) when uplift is just initiated. The critical rotation and displacement are described by Equations 10 and 11 respectively. Substituting the critical rotation into Equation 18 yields the restoring force when uplift is just initiated. This is presented as Equation 19.

$$P_{crit2} = W \frac{R_c \sin\left(\alpha_c - \frac{W}{2k_f B}\right)}{R_c \cos\left(\alpha_c - \frac{W}{2k_f B}\right)} \quad (19)$$

Now consider fixed point ii) when  $\theta = \alpha_c$ , the restoring force reduces to zero and this occurs at a displacement of  $u_{overturn} = R_e [\sin(\alpha_c) + \sin(\alpha_c - \alpha_c)]$ . Combining the results of the two cases, a linear approximation of the restoring force-displacements relationship for displacements after the onset of rocking can be fitted. This is presented as Equation 20,

$$P(u) = \frac{P_{crit2} (u - u_{overturn})}{u_{crit} - u_{overturn}} \quad (20)$$

The results to this point have now effectively mapped the restoring force-displacement characteristics of the rocking system,  $k(u)$ , using a number of closed form formulae. The relationships are summarised graphically in Figure 6.

**Table 1. Model parameters for the numerical validation**

$B$	0.285 m	$H_e$	1.050 m	$k_f$	550 kN/m	$R_b$	0.292 m	$\alpha_b$	77.68 °
$H_b$	0.062 m	$I_{b,g}$	4.33 kgm <sup>2</sup>	$M_b$	44.7 kg	$R_c$	0.836 m	$\alpha_c$	19.93°
$H_c$	0.786 m	$I_{e,g}$	37.57 kgm <sup>2</sup>	$M_e$	122.6 kg	$R_e$	1.088 m	$\alpha_e$	15.18 °

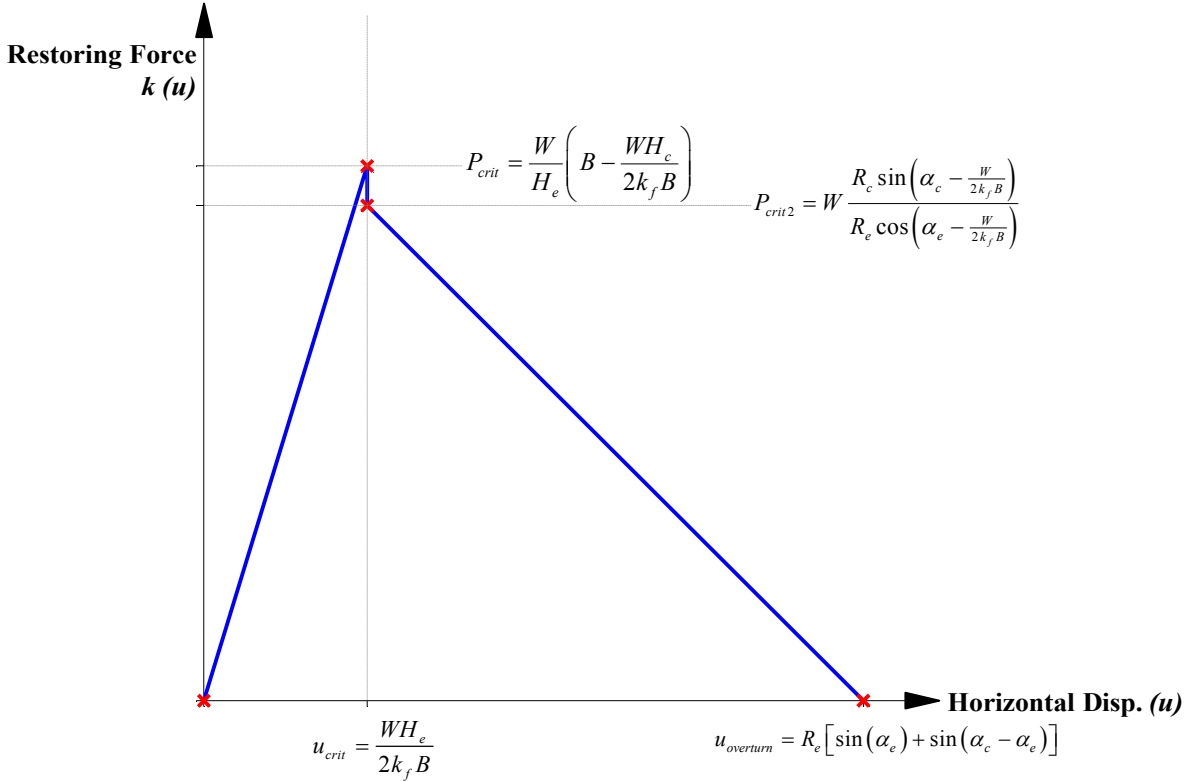


Figure 6: Simplified restoring force-displacement characteristic of a rigid rocking structure on a two-spring foundation.

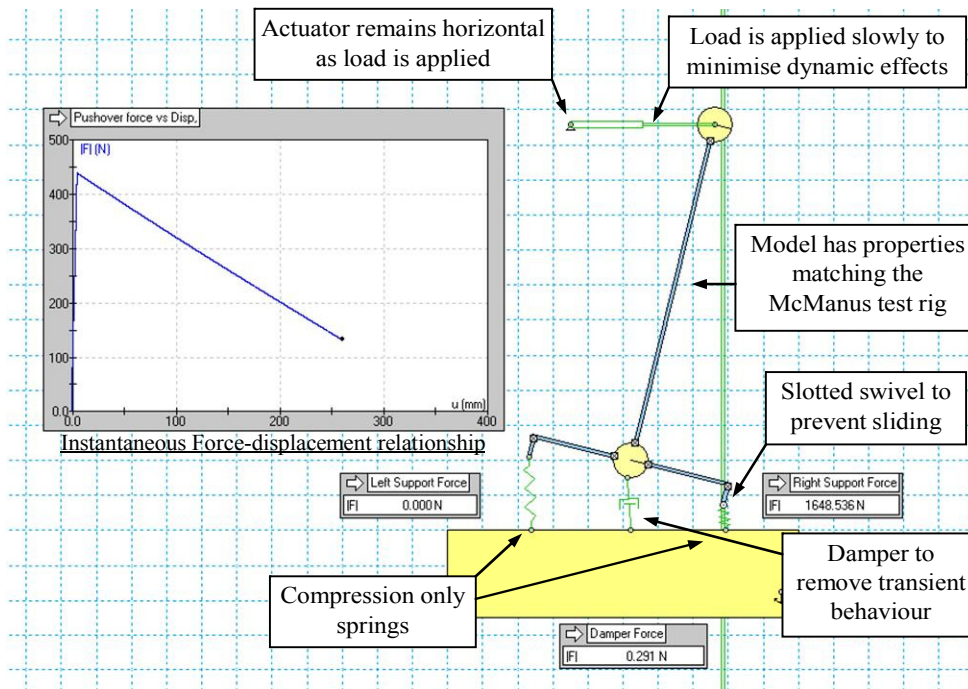
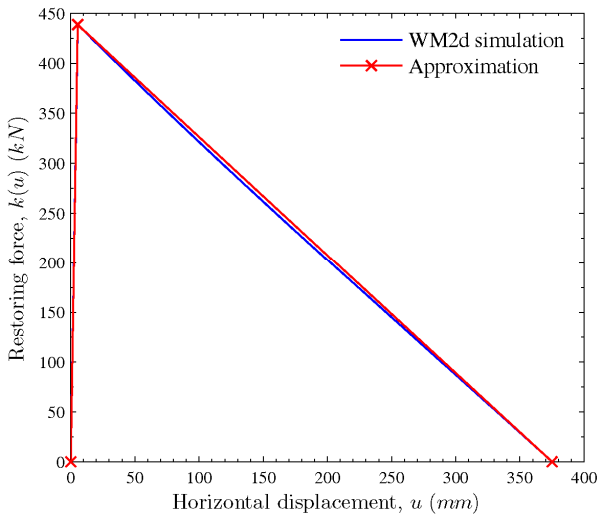


Figure 7: Annotated screenshot of a Working Model 2D analysis.





**Figure 8:** *Nonlinear force-displacement relationship from the proposed approximation formulae and the WM2d simulation.*

These simplified restoring force-displacement relationships were subsequently validated by a computer simulation of a pseudo-static pushover test conducted in Working Model 2D (WM2d) (Design Simulation Technologies 2003), a rigid body dynamic simulation program. The simulation adopted the properties of an uplifting steel column from an experiment by McManus (1980). The key parameters of the specimen are reproduced in Table 1.

An annotated screenshot of the Working Model 2D analysis highlighting some of the modelling features of the computer simulation is presented in Figure 7. Additionally, a comparison of the simulation result and the output of the approximation formula is provided in Figure 8.

This validation exercise clearly demonstrates that the approximation formulae are very accurate across the full range of lateral displacements. Many additional analyses not presented here further confirm the approximation formulae are accurate for a wide range of other structural configurations.

Finally, Equation 11 shows the lateral displacement at which uplift begins is inversely proportional to the spring stiffness ( $k_p$ ). This presents another valuable fixed point with physical relevance which can be exploited to estimate a key parameter of the rocking problem.

## NUMERICAL EXAMPLES

The general behaviour of the proposed simplified SDOF model is demonstrated by two illustrative numerical simulations. The simulations employ the same uplifting steel column in the McManus report described previously as the prototype structure. The analyses simulate the response of the uplifting structure under 1) free vibration decay and 2) earthquake ground motion.

The displacement time-history is predicted in both cases by first evaluating the force-displacement relationship,  $k(u)$ , following Equations 14 through 20, substituting  $k(u)$  into the GDE of motion in Equation 1 and numerically integrating the GDE using an ordinary differential equation solver. During the numerical integration, the algorithm is stopped whenever an impact is detected. Once stopped, the speed of the SDOF model is modified according to Equation 2 and the algorithm is restarted with the new initial conditions. This is repeated until all motion and external forcing has ceased.

Figure 9 presents the simulated displacement time-history adopting this approach for a free-vibration decay test plotted against experimental data extracted from a corresponding test run published previously in the McManus report. Note that the simulation adopted a theoretical  $r$  value of 0.74 following Equation 3.

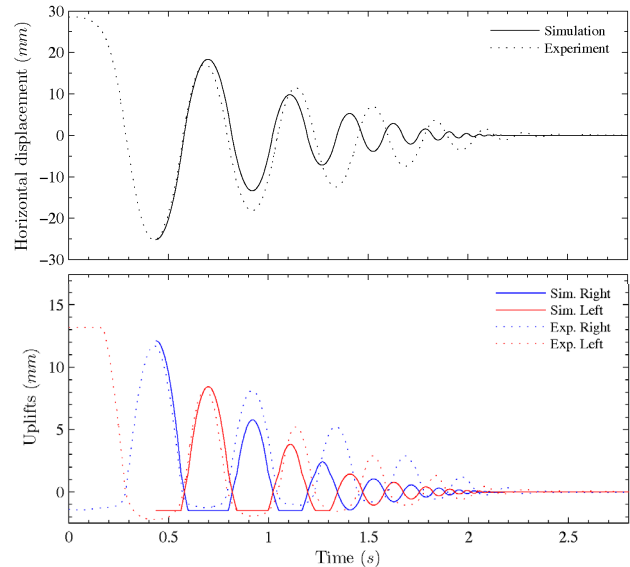


**Figure 9:** *Simulated and actual response of a rocking steel column released from an initial displacement.*

Figure 9 shows that the simplified procedure produced a near perfect displacement prediction from the moment of release until the first impact. This is encouraging as it confirms that it is acceptable to model the rocking problem using the nonlinear SDOF approach based on the two-spring model, and that the proposed approximation equations are accurate. The deterioration of the simulation after the first impact can be attributed to poor emulation of the system's energy dissipation. If the analysis used an empirical  $r$  value higher than the theoretical value, it would improve the overall prediction of the displacement time-history. However this practice would violate the conservation of angular momentum assumption.

It is also of note that the uplift predictions corresponded very well with the experimental uplifts. The simulated uplifts are calculated by converting the horizontal displacements into angular rotations, then by considering rigid body rotation of the structure about the centreline or about the spring in contact, for cases before and after the onset of uplift respectively.

Next, in lieu of accurate experimental validation data, a general demonstration of the isolating effects of permitting rocking is presented. A simulation is conducted subjecting the prototype structure to the 1940 El Centro NS earthquake record. Figure 10 presents the resulting simulated displacement time-histories, and highlights the ability of a rocking system to withstand earthquake motion by swaying in a subdued and stable manner. Note that while the maximum displacement places the system in a region with negative tangential lateral stiffness, the system remained stable and is arguably more isolated from the damaging frequencies of ground motion.

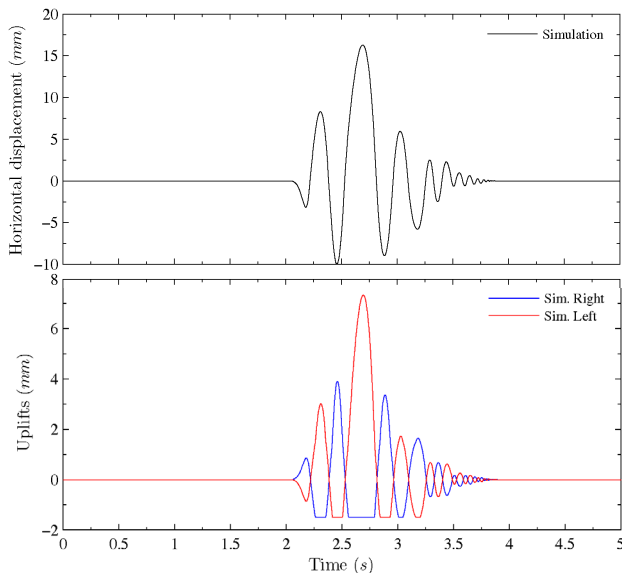


**Figure 10:** Simulated response of a rocking steel column subjected to the 1940 El Centro NS ground motion.

### CONCLUSION

This paper described a new technique to model the dynamic response of uplifting rigid structures subjected to base excitation. The proposed technique exploited the use of a two-spring foundation and developed an equivalent SDOF procedure to model the problem. The two-spring solution made assumptions similar to those in Housner's SRM, but applied them to a rocking rigid structure. The procedure incorporated the effects of foundation flexibility and allowed for a continuous transfer of support forces until uplift.

The key to the simplified procedure was the mapping of the geometrically nonlinear restoring force into a more familiar, pushover nonlinear force-displacement function. A set of simple closed-form approximation formulae was derived employing only basic mechanics principles. The formulae permitted the estimation of the restoring force characteristics using the geometry of the system alone, without the need for a complicated pushover analysis. These formulae were validated using a WM2d simulation, and the result showed the formulae are very accurate across the full range of stable lateral displacements and across a wide range of structural configurations.

The nonlinear force-displacement function was then substituted into the GDE of motion of the equivalent SDOF system. This allowed the dynamic response of the system to be evaluated simply by numerical time-integration.

Finally, this paper presented numerical examples on the use of the proposed procedure to simulate the dynamic response of uplifting rigid structures subjected to base excitation. These examples showed the model produced rational results which compared well with published experimental data.

### REFERENCES

- Anderson, D. L. (2003). "Effect of foundation rocking on the seismic response of shear walls". *Canadian Journal of Civil Engineering*, **30** (2), 360-365.
- Arze, E. (1993). "Seismic design of industrial facilities". *Tectonophysics*, **218** (1-3), 23-41.
- Beck, J. L. and Skinner, R. I. (1974). "Seismic Response of a Reinforced Concrete Bridge Pier Designed to Step". *Earthquake Engineering & Structural Dynamics*, **2** (4), 343-358.
- Chopra, A. K. and Yim, S. C. S. (1985). "Simplified Earthquake Analysis of Structures with Foundation Uplift". *Journal of Structural Engineering*, **111** (4), 906-930.
- Design Simulation Technologies, Inc. (2003). Working Model 2D (6.0.0). Available Distributor: Design Simulation Technologies, Inc., Canton, MI 48187 <<http://www.workingmodel.com>>
- Housner, G. W. (1963). "The behaviour of Inverted pendulum structures during earthquakes". *Bulletin of the Seismological Society of America*, **53** (2), 403-417.
- Huckelbridge, A. A. and Clough, R. W. (1978). "Seismic Response of Uplifting Building Frame". *ASCE J Struct Div*, **104** (8), 1211-1229.
- Ichinose, T. (1986). "Rocking Motion of Slender Elastic Body on Rigid Floor". *Bulletin of the New Zealand National Society for Earthquake Engineering*, **19** (1), 18-27.
- Jennings, P. C. and Bielak, K. (1973). "Dynamics of building-soil interaction". *Bulletin of the Seismological Society of America*, **63** (1), 9-48.
- Kelly, T. E. (2009). "Tentative Seismic Design Guidelines for Rocking Structures". *Bulletin of the New Zealand Society for Earthquake Engineering*, **42** (4), 239-274.
- McManus, K. J. (1980). "The seismic response of bridge structures free to rock on their foundations," *A report submitted in partial fulfilment of the requirements for the degree of Master of Engineering at the University of Canterbury, Christchurch, New Zealand*, University of Canterbury, Christchurch, N.Z.
- Meek, J. W. (1975). "Effects of Foundation Tipping on Dynamic Response". *Journal of the Structural Division*, ASCE, **101** (7), 1297-1311.
- Palmeri, A. and Makris, N. (2008). "Response analysis of rigid structures rocking on viscoelastic foundation". *Earthquake Engineering and Structural Dynamics*, **37** (7), 1039-1063.
- Pampanin, S. (2006). "Controversial aspects in seismic assessment and retrofit of structures in modern times: Understanding and implementing lessons from ancient heritage". *Bulletin of the New Zealand Society for Earthquake Engineering*, **39** (2), 120-134.
- Psycharis, I. N. (1991). "Effect of base uplift on dynamic response of SDOF structure". *Journal of Structural Engineering New York, N.Y.*, **117**(3), 733-754.
- Psycharis, I. N. and Jennings, P. C. (1983). "Rocking of slender rigid bodies allowed to uplift". *Earthquake Engineering & Structural Dynamics*, **11** (1), 57-76.
- Psycharis, I. N., Papastamatiou, D. Y. and Alexandris, A. P. (2000). "Parametric investigation of the stability of classical columns under harmonic and earthquake excitations". *Earthquake Engineering & Structural Dynamics*, **29**, 1093-1109.
- Sharpe, R. D. and Skinner, R. I. (1983). "The Seismic Design of an Industrial Chimney with Rocking Base". *Bulletin of the New Zealand Society for Earthquake Engineering*, **16** (2), 98-106.
- Tse, J., Bryson, J. and Abrahams, M. J. (2002). "Reconstruction of the Lions Gate Bridge Construction Engineering and Methods". 19th annual International Bridge Conference, Pittsburgh, U.S.A.



- Xu, C., and Spyrakos, C. C. (1996). "Seismic analysis of towers including foundation uplift". *Engineering Structures*, **18** (4), 271-278.
- Yim, C. S. and Chopra, A. K. (1984a). "Earthquake Response of Structures with Partial Uplift on Winkler Foundation". *Earthquake Engineering & Structural Dynamics*, **12**, 263-281.
- Yim, S. C. S. and Chopra, A. K. (1984b). "Dynamics Of Structures On Two-Spring Foundation Allowed To Uplift". *Journal of Engineering Mechanics, ASCE*, **110** (7), 1124-1146.
- Yim, S. C. S. and Chopra, A. K. (1985). "Simplified Earthquake Analysis Of Multistory Structures With Foundation Uplift". *Journal of Structural Engineering New York, N.Y.*, **111** (12), 2708-2731.